Robust Proactive Control of Wind Turbines with Reduced Blade Pitch Actuation ⋆

Alexander Stotsky * and **Bo Egardt** **

* *Signals & Systems, Chalmers University of Technology, Gothenburg, SE-412 96, Sweden (e-mail: alexander.stotsky@chalmers.se)*
** *Signals & Systems, Chalmers University of Technology, Gothenburg, SE-412 96, Sweden (e-mail: bo.egardt@chalmers.se)*

Abstract: A new simultaneous speed and pitch control of wind turbines with the preview measurements and look-ahead calculations is considered. The desired piecewise constant pitch angle profile which is calculated using turbine load prediction, allows the reduction of pitch actuation that in turn, increases the lifetime of actuator. The robust collective pitch control architecture with the maximum possible actuation rate is proposed.
Moreover, a new postprocessing technique that provides the high quality estimate of the turbine inertia moment is also described. The results are confirmed by simulation with a wind speed record from the *Hönö* turbine located outside Gothenburg, Sweden.

Keywords: Wind turbine, Robust proactive control, Reduced pitch actuation, Estimation of the inertia moment, Wind turbine icing

1. INTRODUCTION

A stochastic nature of the wind necessitates the development of the preview based control strategies for both maximization of the turbine power and mitigation of the turbine loads [1] - [5]. Preview measurements at a distance in front of the turbine allow preprocessing of the wind speed signal and generation of the high quality wind speed derivative signal, as well as the prediction of future turbine loads and pitch angle. The preview information results in the feedforward part of the control system which is utilized to proactively control the turbine.
Deviations between the wind speed measured at a distance in front of the turbine and the wind speed that arrives to the turbine site as well as inaccurate measurements of the wind speed at the turbine site necessitate the development of robust (with respect to the wind speed measurement errors) control systems.
The proactive turbine control systems are usually based on the expected wind speed i.e., the speed that is measured at a distance in front of the turbine and expected to arrive to the turbine site after some time. A classical frozen turbulence assumption which is used for calculation of the expected wind speed might introduce additional significant inaccuracies in the preview information [4].
Deviations between the expected and actual wind speeds at the turbine site are accounted in the feedforward part of the controller, where only the derivative of the upwind speed signal is used. Therefore the control system is robust with respect to the constant or slowly varying deviations between those two speeds [5]. Besides, a constant error in the derivative of the expected wind speed can be well compensated by the integral term of the feedback turbine speed controller that gives additional robustness to the system.
Unfortunately, the errors in the wind speed measurements at the turbine site, which are delivered by the cup anemometer can not be compensated in the speed control system and usually result in power reduction. However, those errors might be accounted in the pitch control loop within a new load control concept described in this paper. This concept/strategy includes the following three steps: (1) load prediction/calculation is performed using the preview wind speed measurements at the first step ; (2) the desired pitch angle profile is calculated at the second step with a specified upper bound on the flapwise bending moment ; (3) the majorization (overbounding) of the desired pitch angle profile with the piecewise constant function is performed at the third step.
The piecewise constant desired pitch angle profile, which is known in advance, in turn allows : (1) the reduction of the blade pitch actuation ; (2) the design of control system with the high performance tracking capabilities ; (3) the compensation of the errors in the upwind/wind speed measurements as well as inaccuracies due to the frozen turbulence assumption.
Indeed, if the true wind speed at the turbine site is higher than expected and comes with the timing error the turbine loads still satisfy the constraints provided that the piecewise constant upper bound of the desired pitch angle is conservative enough. On the other hand the conservative load regulation with additional power losses can be seen as disadvantage of the proposed approach.
The pitch actuation technique developed in this paper can be seen as extension/robustification of the proactive turbine control method described in [2].
The performance of the blade pitch control system has a direct impact on the turbine mechanical loads. The pitch rate limitation is the most significant factor in the blade pitch actuation. The desired blade pitch angle profile cal-

⋆ This work was supported by the Swedish Wind Power Technology Center

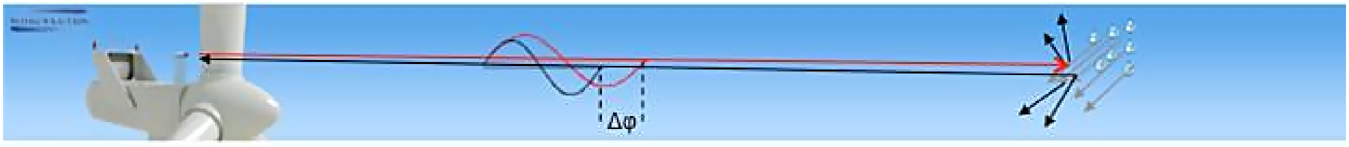

FIG 1. Preview measurements at a distance in front of the turbine. A laser beam (which serves as a reference beam) is focused toward a point which is located at a certain distance in front of the turbine, and a beam (which is a measurement beam) reflected back from dust particles, water droplets, and so on is detected. Wind movements advect particles so that the measurement beam is slightly changed compared to the reference beam. This change is proportional to the wind speed and gives an opportunity for accurate wind speed measurements.

culated in preprocessing is the piecewise constant function of time with available values in preview allows accounting for rate limitation and improves the performance of regulation. The transient between two constant desired values of the blade pitch angle is described as a linear function of time with the rate which corresponds to the maximal blade pitch rate. Availability of the preview information in combination with a spline planning allows the proactive transient of the blade pitch angle with the highest possible rate.
The turbine parameters, such as inertia, drivetrain damping factor and others might change with the turbine operating conditions. Inertia moment, for example changes significantly with ice accretion on the turbine blades in cold climate. Inertia moment can be estimated using turbine model and the generator speed measurements. A noise in the measurements of the generator speed is a main obstacle for real-time estimation of the inertia moment. Postprocessing methods (as alternative methods to real-time estimation) can be used as free tools for the high performance parameter estimation. Postprocessing implies that the turbine signals are saved in the buffer and processed/cleaned using signal processing methods. Preview information in postprocessing might be used for improvement of the estimation accuracy. The prediction error based estimation algorithms with the input signals filtered in postprocessing can be applied for the robust estimation of a slowly varying inertia moment of the turbine.
Main contribution of this paper is twofold: 1) a new robust proactive blade pitch control with reduced actuation; 2) a new postprocessing-based estimation algorithm of the turbine inertia moment.

2. TURBINE MODEL

2.1 Aerodynamic Model

The wind turbine converts energy from the wind to the rotor shaft that rotates at a speed ω_r. The power of the wind $P_{wind} = \frac{1}{2}\rho A V^3$ depends on the wind speed V, the air density ρ, and the swept area $A = \pi R^2$, where R is the rotor radius. From the available power in the swept area, the power on the rotor P_r is given based on the power coefficient $C_p(\lambda, \beta) = \frac{P_r}{P_{wind}}$ which in turn, depends on the pitch angle of the blades β and the tip-speed ratio $\lambda = \frac{\omega_r R}{V}$:

$$P_r = P_{wind}\, C_p(\lambda, \beta) = \frac{A\rho V^3 C_p(\lambda, \beta)}{2} \tag{1}$$

The aerodynamic torque applied to the rotor is given as:

$$T_a = \frac{P_r}{\omega_r} = \frac{A\rho V^3 C_p(\lambda, \beta)}{2\omega_r} \tag{2}$$

2.2 Control Oriented Modeling of the Drive Train

A drive train model consists of a low-speed shaft rotating with a speed ω_r and a high-speed shaft rotating with a speed ω_g, having inertias J_r and J_g respectively. The shafts are interconnected by the gear with ratio N. A torsion stiffness K_s together with a torsion damping K_d result in a torsion angle α that describes the twist of the flexible shaft. This leads to the following drive train model:

$$J_r \dot{\omega}_r = \frac{P_r}{\omega_r} - K_s \alpha - K_d \dot{\alpha} \tag{3}$$

$$J_g \dot{\omega}_g = \frac{K_s}{N}\alpha + \frac{K_d}{N}\dot{\alpha} - T_g \tag{4}$$

$$\dot{\alpha} = \omega_r - \frac{1}{N}\omega_g \tag{5}$$

Assuming that the torsion rate is small, $\dot{\alpha} = 0$, the model (3)-(5) can be reduced as follows [5] :

$$\omega_g = N\omega_r \tag{6}$$

$$J\dot{\omega}_r = \frac{P_r}{N\omega_r} - T_g = \frac{T_a}{N} - T_g \tag{7}$$

where $J = \dfrac{J_r + N^2 J_g}{N}$ is a lumped rotational inertia of the system.
The turbine model (6),(7) can be seen as the control oriented and simplified model, which is suitable and recommended for the control design, whereas the model (3) - (5) can be used for detailed simulations of the turbine response or for the control design for the drive train with essential flexibility of the drive shaft [2].

2.3 Pitch Actuator Model

Pitch actuator is modeled as a first order lag with the rate and range constraints:

$$\dot{\beta} = -\frac{1}{\tau}\beta + \frac{1}{\tau}u_d(t - t_d) \tag{8}$$

$$|\beta| \le C_\beta, \quad |\dot{\beta}| \le C_{\dot{\beta}} \tag{9}$$

where $u_d(t - t_d)$ is an actuator control input, τ is a time constant, t_d is constant and known communication delay, and C_β and $C_{\dot{\beta}}$ are positive constants which define the range and rate constraints respectively.

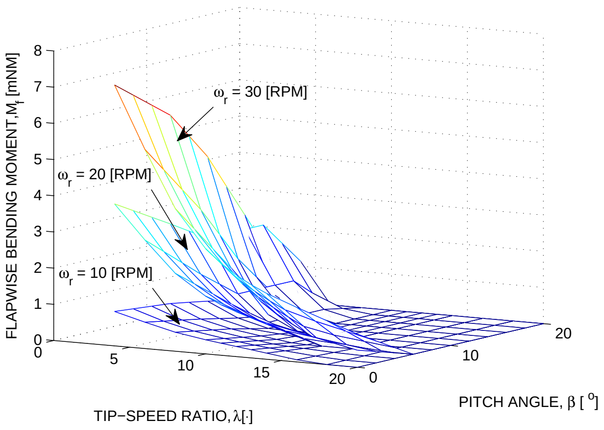

FIG 2. The flapwise bending moment as a function of tip-speed ratio and pitch angle.

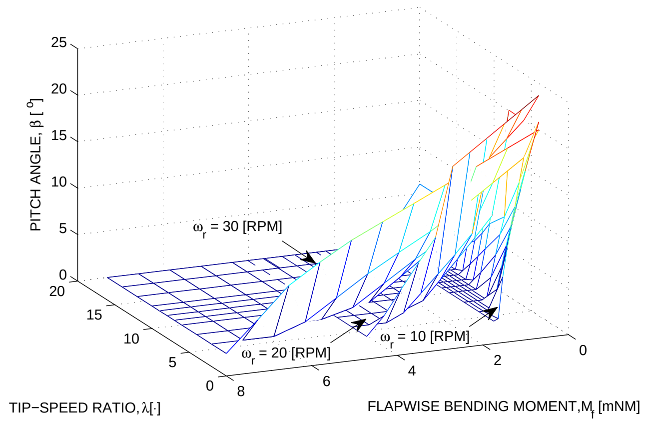

FIG 3. Pitch angle as a function of the flapwise bending moment and tip-speed ratio.

2.4 The Steady-State Blade Operational Loads

A mean value model of the flapwise and edgewise blade root bending moments can be presented in the form of look-up tables (the surfaces in three dimensional space) with the tip-speed ratio and blade pitch angle as input variables. Notice that a wind turbulence introduces fluctuations of the blade loads. However, these fluctuations occur around the mean values of the loads.
The surfaces that describe the flapwise blade bending moment as a function of the tip-speed ratio and blade pitch angle for different turbine speeds are shown in Figure 2. Each of those surfaces can be inverted so that the tip-speed ratio and flapwise bending moment are the input variables and the blade pitch angle is the output variable. Those inverse surfaces are plotted in Figure 3 and can be used for the determination of the desired pitch angle in the flapwise bending moment regulation.

2.5 Wind Speed Measurements

The wind speed measurements made on the *Hönö* wind turbine in Gothenburg, Sweden with the sampling rate of 1 Hz are directly used in simulations. The wind speed measurement setup is described in [5].

2.6 Problem Statement

The turbine control problem statement is to choose the desired generator torque T_g and pitch actuator input u_d in order to track the desired turbine speed ω_{rd}, and blade pitch angle β_d:

$$\lim_{t\to\infty} \omega_r(t) - \omega_{rd} = 0, \tag{10}$$

$$\lim_{t\to\infty} \beta(t) - \beta_d = 0, \tag{11}$$

$$M_f(V, \omega_r, \beta) \le C_f, \qquad C_f > 0, \tag{12}$$

$$M_e(V, \omega_r, \beta) \le C_e, \qquad C_e > 0. \tag{13}$$

where ω_{rd} corresponds to the tip-speed ratio λ_* at the maximum power coefficient and β_d is chosen to satisfy the constraints (12) and (13) on the flapwise $M_f(\cdot)$ and edgewise $M_e(\cdot)$ blade bending moments, respectively. The look-ahead calculation of the desired pitch angle profile β_d is described in Section 3.2.

3. LOOK-AHEAD CALCULATIONS

This Section describes the calculations driven by the upwind speed measurements and divided into two parts. The first part contains a short description of the wind speed derivative estimation technique using spline interpolation method and presented in Section 3.1. This description is carried over from [5]. The second part, described in Section 3.2, involves calculations of the predicted blade loads and generation of the desired piecewise constant pitch angle profile. The results of look-ahead calculations are utilized in Section 4, which describes novel turbine control strategies.

3.1 Preprocessing of Upwind Speed Signal: Calculation of the Derivative

The upwind speed signal measured at a distance in front of the turbine with a relatively low sampling rate (compared to other signals of the system) is processed using spline interpolation method. This method is based on on-line least-squares polynomial fitting over the moving in time window of a certain size. The high quality derivatives of the wind speed signal are calculated analytically and included in the control system as a preview part, see [5] and references therein for details.

3.2 Calculation the Desired Piecewise Constant Blade Pitch Angle Profile

The future/predicted blade loads can be modeled using upwind speed measurements and static maps shown in Figure 2. The desired pitch angle profile is calculated using the surfaces which are inverse to the flapwise bending moment surfaces. Those inverse surfaces are shown in Figure 3 with the desired flapwise bending moment and upwind speed as input variables. The desired pitch angle profile, calculated via the inverse surfaces guarantees that the flapwise bending moment will not exceed the desired upper bound.

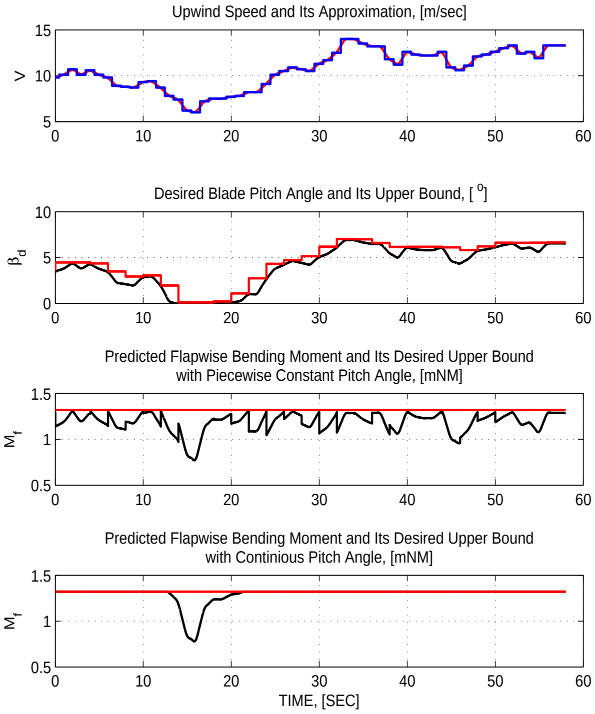

FIG 4. The time chart of look-ahead calculations. The upwind speed is shown in the first subplot with a blue line together with its spline approximation plotted with a red line. The desired pitch angle profile and its upper bound are plotted as black and red lines respectively in the second subplot. The flapwise bending moment is plotted in the third and fourth subplots with a black line for continuous and piecewise constant pitch angle profiles respectively. A desired flapwise bending moment is plotted with a red line.

The time chart of look-ahead calculations is shown in Figure 4. All the calculations are driven by the upwind speed shown in the first subplot with a blue line together with its spline approximation plotted with a red line. The desired pitch angle profile calculated using the approach described above is plotted with a black line in the second subplot. This profile guarantees that the flapwise bending moment does not exceed a pre-specified upper bound as it is shown in the fourth subplot, where the bending moment is plotted with a black line and its upper bound is plotted with a red line.

Finally, Figure 2 shows that larger pitch angles imply lower bending moments at a fixed turbine speed. Therefore, overbounding of the desired pitch angle profile with the piecewise constant function of time guarantees that the flapwise bending moment does not exceed a pre-specified upper bound. An upper bound of the desired pitch angle is plotted with a red line in the second subplot of Figure 4. The corresponding flapwise bending moment is plotted with a black line in the third subplot, and its upper bound is plotted with a red line.

The look-ahead calculations result in the desired piecewise constant blade pitch angle profile with available values in preview (future values) that allows the design of a new robust turbine load control system with improved performance, see Section 4.2.

4. NOVEL TURBINE CONTROL STRATEGIES

This Section starts with the description of the turbine speed control strategy with the derivative of upwind speed signal, described in Section 3.1. A novel rapid blade pitch angle control strategy is described in Section 4.2. Finally, a new technique for estimation of the inertia moment is presented in Section 4.3.

4.1 Turbine Speed Control

The robust control strategy that uses the calculated ahead derivative of the wind speed signal can be written as follows [5]:

$$T_g = \underbrace{\frac{P_r}{N\omega_{rd}}}_{feedforward\ part} - \underbrace{J\dot{\omega}_{rd}}_{preview\ part} \underbrace{+ \gamma_r\ (\omega_r - \omega_{rd}) + \gamma_{r1} \int (\omega_r - \omega_{rd})}_{feedback\ part}, \tag{14}$$

where the desired turbine speed $\omega_{rd} = \frac{\lambda_* V}{R}$ is driven by the wind speed V measured at the turbine site, and the derivative of the desired turbine speed $\dot{\omega}_{rd} = \frac{\lambda_* \dot{V}_p}{R}$ depends on the upwind speed derivative $\dot{V}_p$, cleaned from the noise in the preprocessing and time shifted according to the frozen turbulence assumption. The turbine speed is calculated via generator speed $\omega_r = \frac{\omega_g}{N}$, and the feedback gains γ_r and γ_{r1} in (14) are positive.

Notice that the derivative of the desired turbine speed $\dot{\omega}_{rd}$ plays the role of the preview part in the control action (14) and essentially improves the performance of the regulation. Integral part of the controller compensates errors in the derivative of the expected wind speed.

This strategy, when combining (7) with (14), results in the following closed loop system:

$$\dot{\tilde{\omega}}_{r1} = \tilde{\omega}_r \tag{15}$$

$$J\dot{\tilde{\omega}}_r = -[\frac{P_r}{N\omega_r\ \omega_{rd}} + \gamma_r]\tilde{\omega}_r - \gamma_{r1}\tilde{\omega}_{r1} \tag{16}$$

where $\tilde{\omega}_r = \omega_r - \omega_{rd}$. This model represents a stable dynamics and the turbine speed converges to the desired speed with the guaranteed performance [5].

The Lyapunov function candidate $Q = \frac{J}{2}\tilde{\omega}_r^2 + \frac{\gamma_{r1}}{2}\tilde{\omega}_{r1}^2$, with the following derivative along the solutions of (15) and (16) $\dot{Q} = -[\frac{P_r}{N\omega_r\ \omega_{rd}} + \gamma_r]\tilde{\omega}_r^2$ can be used for the proof of the system stability.

Notice that the turbine model (6),(7) is used for the control design, whereas the model (3) - (5) is used for simulations. Simulation results of the turbine response with the control action (14) and model (3) - (5) is shown in the third subplot of Figure 6.

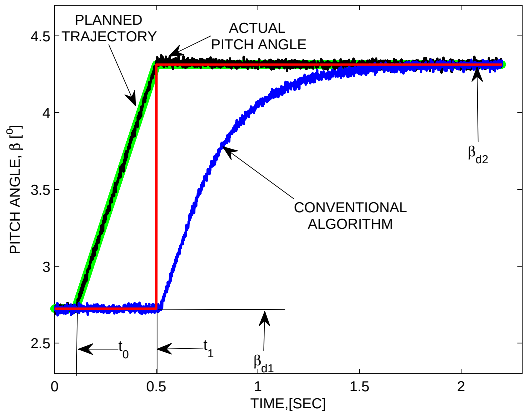

FIG 5. The proactive transient between two desired pitch angles (β_{d1} and β_{d2}), plotted with a red line. The transient response for the conventional algorithm is plotted with a blue line. The planned desired transient trajectory is plotted with a green line, with the transient start and stop times t_0 and t_1 respectively. The response of the pitch actuator driven by control algorithm (17) is plotted with a black line.

Notice that the rotational inertia of the system J can be seen as the significant weighting factor to the upwind speed derivative $\dot{V}_p$ that quantifies the contribution of the preview information in the control algorithm (14). Inertia of the system might drastically change in cold climate with ice accretion on the turbine blades, that introduces errors in the preview information and hence deteriorates the tracking performance of the system. This in turn, necessitates the development of the estimation algorithm based on the generator speed measurements and the turbine model for correction of the values of inertia moment. Noisy measurements of the generator speed is one the main obstacles for the real-time high performance estimation. Therefore, the postprocessing estimation of the inertia moment, described in Section 4.3 is proposed in this paper that improves robustness of the turbine speed control system.

4.2 Rapid Proactive Control of the Blade Pitch Angle

The desired blade pitch angle profile, calculated using upwind speed measurements (see Section 3.2) is a piecewise constant function of time with available values in preview (future values). This allows the design of a high performance pitch regulation system with the highest possible transient rate, used in the algorithm as a parameter.
The transient between two constant desired values of the blade pitch angle is described as a linear function of time with the rate which corresponds to the maximum blade pitch rate $C_{\dot{\beta}}$. This linear function can be seen as a spline that describes the shortest feasible path between the two constant desired values. The desired trajectory $C_0 + C_{\dot{\beta}} t$ in the transient between two constant values β_{d1} and β_{d2}, ($\beta_{d2} > \beta_{d1}$) is defined as follows:

$$\beta_d = \begin{cases} \beta_{d1} & \text{if } t < t_0 \\ C_0 + C_{\dot{\beta}} t & \text{if } t_1 \geq t \geq t_0 \\ \beta_{d2} & \text{if } t > t_1 \end{cases}$$

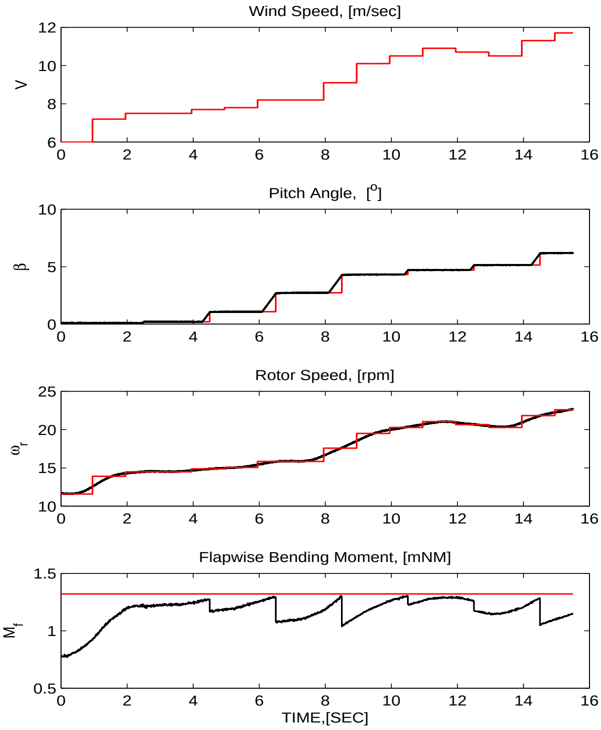

FIG 6. The time chart of the wind speed (red line in the first subplot), the desired and actual pitch angles (red and black lines respectively in the second subplot), the desired and actual rotor speeds (red and black lines respectively in the third subplot) and the flapwise bending moment (black line in the fourth subplot) of the forward looking control strategy.

where the start time of transient t_0 together with the constant C_0 are calculated for the prescribed values of the rate limit $C_{\dot{\beta}}$ and the stop time of transient t_1, see Figure 5. Availability of the preview information in combination with the spline planning allows the advance start of the transient that occurs with the highest possible transient rate (used in algorithm as the parameter) at the prescribed stop time.
The transient control action for the blade pitch actuator, compensated for the time delay t_d, is defined as follows [5]:

$$u_d = \underbrace{(C_0 + C_{\dot{\beta}} t)}_{= \beta_d} + \tau \underbrace{C_{\dot{\beta}}}_{= \dot{\beta}_d} \tag{17}$$

which in combination with (8) results in the following exponentially stable closed loop dynamics:

$$\dot{\beta} - \dot{\beta}_d = -\frac{1}{\tau}(\beta - \beta_d) \tag{18}$$

Notice that the time constant of the pitch actuator might change with operating conditions. A priori value of the time constant is used in this case in algorithm (17) that does not significantly deteriorate the control system performance.
Figure 5 shows the comparison of two responses of the blade pitch actuator with the control action (17) and the conventional control action $u_d = \beta_d$ for the piece-

wise constant β_d without any preview information. The transient response of the system with algorithm (17) is essentially better than the response of the system with the conventional control action due to availability of the preview information and proactive planning.
Finally, the performance of simultaneous speed and pitch control (14) and (17) is illustrated in Figure 6. The wind speed record is shown in the first subplot, the performances of the pitch and speed controls are shown in the second and third subplots respectively, and finally the corresponding flapwise bending moment is shown in the fourth subplot.

4.3 Estimation of the Inertia Moment in Postprocessing: Prediction Error Based Approach

Inertia moment can be estimated using measurements of the generator speed ω_g and turbine model (7), which can be written in the following form:

$$\dot{\omega}_g = \theta_* \varphi \tag{19}$$

where $\varphi = N(\frac{P_r}{\omega_g} - T_g)$ is the regressor and $\theta_* = \frac{1}{J}$ is unknown parameter. The prediction error based estimator is defined as follows [6] :

$$\dot{\psi} = -\alpha_0 \psi - \varphi, \qquad \psi(0) = 0,\ \alpha_0 > 0, \tag{20}$$

$$\dot{\varepsilon} = \alpha_0(\omega_g - \varepsilon) + \varphi\theta - \psi\dot{\theta}, \qquad \varepsilon(0) = \omega_g(0), \tag{21}$$

$$\dot{\theta} = -\gamma_e \psi(\omega_g - \varepsilon), \qquad \gamma_e > 0, \tag{22}$$

where θ is an estimate of θ_*, and ψ and ε are auxiliary filters. Evaluation of the variable $\omega_g - \varepsilon - \psi\tilde{\theta}$, where $\tilde{\theta} = \theta - \theta_*$ yields:

$$\frac{d}{dt}[\omega_g - \varepsilon - \psi\tilde{\theta}] = -\alpha_0(\omega_g - \varepsilon - \psi\tilde{\theta}) \tag{23}$$

and hence $\omega_g(t) - \varepsilon(t) - \psi(t)\tilde{\theta}(t) = (\omega_g(0) - \varepsilon(0) - \psi(0)\tilde{\theta}(0))e^{-\alpha_0 t} = 0$ due to the proper choice of the initial conditions. Therefore the variable $\omega_g - \varepsilon$ can be used instead of the prediction error $\psi\tilde{\theta}$, and estimator (22) be written as

$$\dot{\tilde{\theta}} = -\gamma_e \psi^2 \tilde{\theta} \tag{24}$$

The regressor φ is bounded away from zero in the turbine transient operation. This in turn implies that ψ is also bounded away from zero, which guarantees the convergence of the estimated inertia to the true inertia moment. Unfortunately, this high gain estimator is sensitive to the generator speed measurement noise and its application in real-time gives a noisy estimate of the inertia moment. High quality estimation is achieved in the case of post processing, after cleaning of the noisy generator speed measurements. Generator speed measurements are saved in the buffer and approximated via a polynomial in a moving in time window in the least-squares sense. A filtered value of the generator speed is memorized in the middle of the moving window. The performance of postprocessing estimation of the inertia moment is illustrated in Figure 7. Estimated inertia moment $\frac{1}{\theta}$ is used in the control strategy (14) for improvement of the performance of the turbine speed regulation.

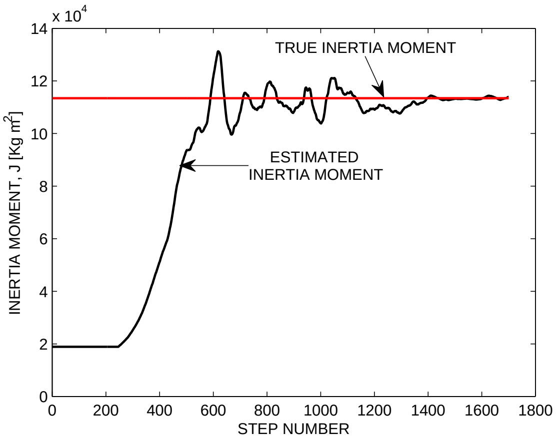

FIG 7. Postprocessing estimation of the inertia moment. The estimated inertia moment is plotted with a black line and true inertia is plotted with a red line.

5. CONCLUSION

A new robust proactive pitch control strategy with the maximum possible actuation rate is proposed. The desired blade pitch angle profile, calculated in preprocessing using preview measurements is the piecewise constant function of time that allows the reduction of the pitch actuation, that in turn saves energy and increases the lifetime of actuator. Moreover, the postprocessing technique of the estimation of the inertia moment, developed in this paper allows exact estimation of the mass of the blade ice that guarantees safe and stable turbine operation in cold climate.

REFERENCES

[1] Laks J., Pao L., Wright A., Kelley N. and Jonkman B., The Use of Preview Wind Measurements for Blade Pitch Control, Mechatronics, 21, 2011, pp. 668-681.

[2] Stotsky A. and Egardt B., Proactive Control of Wind Turbine with Blade Load Constraints, Proc. IMechE Part I: Journal of Sytems and Control Engineering, vol. 226, N 7, August 2012, pp. 985-993.

[3] Wang N., Johnson K. and Wright A., FX-RLS-Based Feedforward Control for LIDAR-Enabled Wind Turbine Load Mitigation, IEEE Transactions on Control Systems Technology, vol. 20, N 5, September 2012, pp. 1212-1222.

[4] Simleyz E., Pao L., Kelley N., Jonkman B., Frehlich R., LIDAR Wind Speed Measurements of Evolving Wind Fields, The 50-th AIAA Aerospace Sciences Meeting, 09 - 12 January 2012, Nashville, Tennessee, USA, AIAA 2012-0656. pp. 1 - 19.

[5] Stotsky A. and Egardt B., Model Based Control of Wind Turbines: Look-Ahead Approach, Proc. IMechE Part I: Journal of Sytems and Control Engineering, vol. 226, N 8, September 2012, pp. 1029-1038.

[6] Stotsky A., Lyapunov Design for Convergence Rate Improvement in Adaptive Control, International Journal of Control, vol.57, No 2, 1993, pp. 501-504.